Ocean Sci. Discuss., 10, 1559–1580, 2013
www.ocean-sci-discuss.net/10/1559/2013/
doi:10.5194/osd-10-1559-2013

Ocean Science
Discussions
Open Access

Observations of phytoplankton spring bloom onset triggered by a density front in NW Mediterranean

A. Olita[1], S. Sparnocchia[3], S. Cusí[2], L. Fazioli[1], R. Sorgente[1], J. Tintoré[2], and A. Ribotti[1]

[1]CNR-IAMC, Institute for Coastal Marine Environment, Oristano Section, Italy
[2]SOCIB, Balearic Islands Coastal Observing and Forecasting System, Spain
[3]CNR-ISMAR, Institute of Marine Sciences, Trieste Section, Italy

Received: 5 August 2013 – Accepted: 8 September 2013 – Published: 11 September 2013

Correspondence to: A. Olita (antonio.olita@cnr.it)

Published by Copernicus Publications on behalf of the European Geosciences Union.

Abstract

Phytoplankton bloom in NW Mediterranan sea is a seasonal event that mainly occurrs in a limited area (Gulf of Lyon and Provençal basin) where this phenomenon is promoted by a cyclonic circulation, strong wind-driven mixing and subsequent spring restratification. At the southern boundary of this area a density front (North Balearic Front) separating denser waters from the lighter Modified Atlantic Waters reservoir at south is suspected to trigger weaker and earlier (late winter) blooms by (a) enhanced pumping of nutrients into the euphotic layer and (b) promoting an early restratification of the water column (by frontal instabilities). A multisensor glider round trip, equipped with CTD and fluorimeter, crossing the frontal area in February–March 2013, allowed to observe the bloom triggering after the decrease of intense wind-driven turbulent convection and mixing. Satellite imagery supports and confirms in-situ observations. It was shown that frontal activity has a relevant role in the promotion and acceleration of the dynamical restratification, with a consequent biological response in terms of primary production. Restratification is necessary preconditioning factor for bloom triggering in frontal area, net of other involved mechanism promoting the bloom as the enhanced biological pump. So, like for high-latitude fronts (Taylor and Ferrari, 2011a), also for this mid-latitude oligotrophic region front seems to promote new production by dynamically enahnced restratification inhibiting mixing. Finally, we argued that Sverdrup's Critical Depth criterion seems to apply in the northern well-mixed area, where the zeroing of heat fluxes (and related turbulent convection) does not correspond to a prompt onset of the bloom (which appeared 1 month later).

1 Introduction

A debate is underway in the oceanographic community about the physical/ecological mechanisms triggering the seasonal phytoplankton bloom in seas and oceans at different scales. Some authors (Huisman et al., 1999; Behrenfeld, 2010; Taylor and Ferrari,

2011b; Martin, 2012) recently refused/revised the validity of the classical Critical Depth (CD) hypothesis (Sverdrup, 1953) formulated at global/basin scales. The CD hypothesis, formalized by Sverdrup (1953), in practice states that when the mixed layer depth (MLD) is shallower than the CD, assuming favourable environmental conditions (sufficient light and that loss < growth), the bloom is triggered and maintained thanks to the residence, persistence and growth of phytoplanktonic populations into the euphotic layer (i.e. in these conditions light is NOT a limiting factor). The point is that the CD hypothesis assumes a homogeneous vertical distribution of the phyhtoplankton in the water column, a situation that can be recorded only for well mixed layers.

Behrenfeld (2010) openly (from the title) contested the validity of the CD hypothesis opposing, on the basis of satellite series and in situ biomass records in North Atlantic, a Dilution-Recoupling hypothesis focused on the balance between growth and loss, where loss is mainly grazing. On the other hand Taylor and Ferrari (2011b), extending the work of Huisman et al. (1999) which first opposed the concept of Critical Turbulence (CT) to the Sverdrup's CD, found that the primary engine is the atmospheric forcing (turn off of wind forcing) as in the Sverdrup hypothesis, but the regulating factor is the reduction of vertical turbulence (vertical convection) and not the shoaling of the ML. It has to be underlined that Taylor and Ferrari (2011b) focused their attention to the turbulence generated by surface cooling, therefore to the heat fluxes driven convection, while the contribution to turbulence due to momentum was not investigated. The latter could have an important role for a fullfilling explanation of the CT hypothesis.

Despite the different criteria (critical depth or turbulence) to evaluate/predict the timinig/strength of bloom triggering, the rationale is quite similar between the two hypotheses as the condition to be respected is the persistence of the phytoplanktonic cells in the euphotic layer operated by physical processes. Chiswell (2011) also called in question the CD hypothesis, showing that it cannot be applied in spring because the uneven plankton distribution in the ML, but stating that should not be abandoned completely as it applies when plankton is well mixed throughout the ML (autumn–winter). Bernardello et al. (2012), trough a coupled physical-biological model, also supported

the Huisman-Taylor's CT hypothesis, describing the heat fluxes reduction (in an area of NW Mediterranean characterized by deep ML and strong seasonal bloom) as a better predictor for the bloom onset than the shallowing of the Mixed Layer.

In this main framework, fronts are key environments as they are well known regions of particular high productivity at meso-scale and sub-mesoscale. The presence of fronts and other mesoscale features further complicate the scenario about the forcings (and limiting factors) of the seasonal bloom. Taylor and Ferrari (2011a), in a paper about the role of fronts in the primary production of high-latitude regions, show that frontal restratification inhibits vertical mixing favouring the bloom. Weak mixing reduces the flux of phytoplankton cells out of euphotic zone. This could be a relevant process also in oligotrophic regions at mid-latitudes. Some authors (Lévy et al., 2001; Mahadevan and Tandon, 2006; Lévy, 2008) also showed that sub-mesoscale cyclones and density fronts may promote primary production by increasing the upwelling of nutrients in the photic layers in virtue of very large vertical velocities. Analogously, Mahadevan et al. (2012) show that in North Atlantic, at high latitude, the stratification required for triggering the seasonal bloom often is not initiated by the seasonal warming but is due to Eddy instabilities in areas of strong density gradients. Such instabilities, in absence of strong wind forcing, cause lighter water stratifies over denser water even in absence of heating. Apart the tipology of feature analysed (eddy vs. front) the mechanism is similar to the one proposed for high latitude fronts. Lévy et al. (2012), in their review on submesoscale and blooms, notes that from an observational point of view we have now at disposal oceanographic instruments like gliders and other UAV capable to resolve sub-mesoscale processes even under critical environmental conditions (storms).

In this work we observed that also at mid-latitude, for oligotrophic areas like the Balearic sea is, the early restratification promoted by a density front (the North Balearic Front, NBF hereafter) plays a crucial role in determining the early initiation of the bloom. We studied the NBF area (NW Mediterranean) during the early-bloom period (late winter). The study was conducted through a set of hydrologic and fluorimetric data collected during a glider mission completed in February–March 2013 under the JERICO

Trans National Access program. The glider performed a round trip between Balearic and Sardinia islands (Fig. 1). The analysis of in situ data was supported by satellite Ocean color synoptic data and by auxiliary modelled data.

2 Materials, methods and data

The glider technical specifications, data used and the analyses performed are described in this section.

2.1 Glider technical specifications and hydrological data

The glider used for the experiment was a Seaglider™ 1KA (Eriksen et al., 2001) manufactured by iRobot. The Seaglider™ uses a buoyancy engine to alter its overall density, allowing for vertical displacement through the water column. While moving vertically, its wings produce a lift effect that provides outward propulsion. The batteries, weighting approximately 10 kg (20 % of the glider total weight), shift inside, so that glider pitch, roll and heading can be modified. The result is a sawtooth navigation pattern characteristic of these autonomous vehicles. To reach the programmed waypoints, the glider uses the mechanisms described, a compass that measures altitude and heading and a GPS receiver. Every time the Seaglider ends a dive, it surfaces, obtains a GPS fix and computes the Depth Average Current it just encountered allowing to correct its course and eventually reach the next waypoint. Then, it connects to the land server (base station) through the Iridium satellite network to download new commands to be executed during next dive. Before diving again, it sends scientific and technical data collected during previous dive. For this mission, the Seaglider was configured to dive and climb at a vertical velocity of about 10 cm s^{-1} and to move horizontally, without taking into account currents, at approximately 17 cm s^{-1}. Pitch angle was about 20 degrees and depth range, when the bathymetry allowed, was 0–1000 m. The glider was equipped with a SeaBird CT-Sail (S/N 0173) – a free-flushed device – last calibrated in March

2011. To measure depth, a Paine Electronics pressure sensor (S/N 264065), last calibrated in February 2011, was used. The glider acquired CTD data once every 4.6 s (approximately 0.46 m) along the entire depth range. The data was post processed by the University of Washington's python code that computes conductivity, temperature, salinity, and potential density from the raw values. Glider Matlab Toolbox (Garau et al., 2011) was applied to the data to correct the usual lags found in CTD data. In particular, as an un-pumped CTD has been used, the data were affected by a thermal-lag which has been corrected through this toolbox. Salinity and temperature profiles have been divided in outward and return trip: in that way the interpretation of structures and processes occurring during the cruise was simpler. Both ascending and descending profiles have been used. Densities have been interpolated on a regular grid having horizontal and vertical resolutions of about 2 km and 1 m, respectively. This was done in order to better estimate the ML depth by using the interpolated densities. ML depth was estimated for both eastward and westward transects by using a threshold method: the ML lower limit was identified as a density increase larger than 0.2 kg m^{-3}, referred to the (sub-)surface value. The glider mounted a WET Labs ECO Triplet fluorometer (S/N BBFL2VMT-777) capable of measuring fluorescence and (derived) Chlorophyll *a*. The sensor, last calibrated in November 2010, has a resolution of 0.012 µg L^{-1}. During the first week it sampled the 0–300 m depth range and, to minimize consumption, since then the depth range was reduced to 0–180 m. Once the eastward section was achieved, it was decided to sample one out of four dives as the energy consumption was still too high. During the entire mission, the sensor was sampling every 9.2 s approximately, which translates to a sample every 0.92 m. Chlorophyll *a* (Chl *a* hereafter) is retrieved by linear scaling using regression parameters (slope and intercept) as provided by the manufacturer.

2.2 Other data

A heterogeneous (modelled and satellite) dataset was used to support glider observations and correctly interpret the results.

Ocean-Color 1 km data are Level-2 (single swaths) acquired from MODerate resolution Imaging Spectro-radiometer (MODIS) sensor on board of the AQUA mission and downloaded from the oceancolor web portal (http://oceancolor.gsfc.nasa.gov). The Level-2 MODIS data have been post-processed and mapped by using SEADAS™ software. These data were used to qualitatively compare glider results with synoptic satellite observations helping in the correct interpretation of results.

Surface heat fluxes are extracted from the Western Mediterranean Regional Model, which is the Princeton Ocean Model (POM, Blumberg and Mellor, 1987) operational implementation for the Western Mediterranean, daily providing 5 days forecasts of currents and other relevant ocean variables in Western Mediterranean (www.seaforecast.cnr.it). Heat fluxes are computed by using the well known bulk formulae (Castellari et al., 1998). We assume for convention that heat fluxes are positive when the sea surface is gaining heat. Wind stress data has been also extracted from the model outputs. Wind intensities and directions hourly data were extracted from Skiron forecasts (Kallos et al., 2005) over the period and area of the glider round trip. The 1st day of forecast was used to build the series, in order to obtain a series with the lowest uncertainity.

3 Results

3.1 Dynamical features and Chl *a*

The glider sampled the planned round trip in about 40 days, from 31 January to 9 March 2013, collecting salinity and temperature up to 1000 m depth and Chl *a* (fluorescence, scaled to Chl *a*) up to 180 m (300 m during the first seven days).

In Fig. 2 outward and return sections for temperature and salinity up to 600 m depth are presented. At first glance, the stratification (and the MLD) of the area (both for outward and return trip) is subject to a large variability throughout the glider path. This is the typical signature related to an intense mesoscale activity. Deep ML areas alternating to shallower ones, with isosurface strongly sloped, suggest a sequence of

convergence and divergence zones typical of the (sub-)mesoscale instabilities (frontal meanders and eddies). More in detail, along the outward trip the most evident feature is a large region (between ∼ 5 and ∼ 6° E) characterized by a deep and well mixed upper layer (between 100 and 150 m, see Fig. 3). Here the temperature is about 14.3 °C and a relative minimum of salinity of ∼ 37.8 was found, a value indicating the presence of Modified Atlantic Water, MAW (e.g. Ribotti et al., 2004). Chl *a* concentration is lower than 1 mg m^{-3} and uniformely distributed throughout this deep ML. Satellite imagery (Fig. 4) does not put in evidence any coherent mesoscale eddy, so the generation of such a deep mixing should be due to the wind forcing the reservoir of MAW south of the NBF. The ML depth we estimated from derived densities is in agreement to the Ekman Layer depth calculated empirically from the wind speed blowing in that period (see Fig. 5).

East of this area, at about ∼ 6.8° E, a narrow region characterized by upwelled cold and salty waters was detected in the outward transect. This upwelling is due to the divergence area produced by the proximity of two anticyclones, labeled A1 and A2 in Fig. 4. Satellite image clearly shows the presence of this two eddies, A1 located between ∼ 6 and ∼ 7° E and A2 between ∼ 7 and ∼ 8° E. In glider sections, A2 is caught with the typical inverse-bell shape of the isosurfaces, with the MLD sinking in correspondence of the center of the eddy and shoaling at its margins. This is less evident in A1, at least in *T* and *S*, while densities (Fig. 3) shows this typical shape. The eddies were also detected in the return trip (see bottom panels of Figs. 2 and 3) even if their vertical shape is quite changed, above all for A1. This could be due both to eddies movement on the domain as well as to the slightly different path of the glider. In A2 it is evident that the core of MAW, confined only in the western arm of the eddy during the outward glider trip, was captured also by its eastern arm in the return. Comparing the two sections drawn by outward and return trips, the eddy is wider in the first transect and more stretched to the Sardinian continental slope in the second. This is probably because A2 was matched, in the return trip, in its periphery. This fact is also confirmed by the Chl *a* distribution related to A2.

In both outward and return sections, it is worth of notice the presence of an underlying Levantine Intermediate Waters core (LIW, see for instance Millot and Taupier-Letage (2005)) flowing along the continental margin of the western Sardinia between 300–600 m ($\theta = 14.3\,^{\circ}$C and $S = 38.6$–38.8). The LIW core shape is strongly modified by action of the eddy activity. In particular, comparing the outward and return trip signatures of this structure, it is evident that the LIW core is uplifted from 300–400 m to about 200 m by the eddy activity. Another LIW signal (a little modified in respect to the former) is detected in the middle of the outward transect, probably associated to the transport performed by the other eddy (A2) that was not matched by the glider but that is visible from satellite image in Fig. 4. This second LIW core seems to disappear (mixed or unmatched) in the return trip of the glider. The previously cited deep ML found at the begin of February completely disappeared when the glider came back in the same area 1 month later (cfr 5 February to 5 March). In March the warm-core of the previously seen anticyclonic meander is now considerably cooled, assuming values similar to surrounding water masses. This strong cooling, operated by the severe wind events occurred during the period (Fig. 2), determined a parallel increase in the surface water densities. This, however, did not generate a deeper mixed layer, as the underlying intermediate layer is characterized by heavy and salty waters (the modified LIW), which creates a haline-based stratification opposing a strong resistance to mixing. Therefore, notwithstanding the occurred cooling and the thermal homogeneity of the water column, the ML in this area is shallower at the begin of March than during the outward trip, because of an uplift of the isopycnals (see Fig. 3). Despite the shoaling of the ML, we did not observe in this area a clear biological response in respect to the outward trip. Probably, from a biological perspective, the ML is still quite deep (70–90 m) in this area, even if turbulent convection is already reduced by a zeroing of surface heat fluxes (Fig.6). On the contrary, the MLD shoals above 40–50 m only at the extreme western margin of the return transect. Here (between ~ 4.5 and $\sim 5^{\circ}$ E) the shoaling is due to an increase of density which is maximum for the 40–120 m layer. The increase in density is relative to a water column that, in February, was almost completely uniform

from sub-surface (~ 10 m) to 120 m. In March this shoaling of the ML corresponds to a clear biological response: the Chl *a* increases in the frontal area between ~ 4.5 and $\sim 5^{\circ}$ E up to 2.5 mg m^{-3}. This shoaling is likely to be operated by the instabilities of the front itself: it is evident from satellite image that the area where the bloom onset occurs is coincident with a frontal meander. Here, accordingly to Taylor and Ferrari (2011a), frontal instabilities promote the re-stratification of the water column when the wind forcing is sufficiently low to lower turbulent mixing. The buoyancy (Brunt-Väisälä) frequency is also shown in Fig. 3. It helps in finding out and distinguish areas characterized by strong stratification (red) from well mixed regions. Features visible in terms of buoyancy fit quite well with the MLD identified with the density criterion. It is evident the increased surface stratification in the frontal area (left side of the plots) in the return trip in respect to the outward one, as well as the break-out of the deep-stratification that was present in the outward trip in the frontal region related to the deep thermocline.

3.2 Bloom triggering mechanism

The biological response consequent to the shoaling of the ML in the frontal area is effective before we have a proper thermal re-stratification. The event is recorded few days after the change of sign of the surface heat fluxes (Fig. 6). After the shutdown of NW (cold) winds forcing and in correspondence of a considerable event of southern (warm) winds, the winter cooling of sea surface was interrupted at the beginning of March. In correspondence of this inversion of sign, the area where the front insists started to re-stratify. This early re-stratification, in respect to surrounding areas, determines the reduction of the possibility for upper euphotic layers to mix with underlying a-photic water masses. It is worth of notice that the same spatial/temporal pattern of heat fluxes occurs both along the glider path (crossing the front) as well in the middle of the MEDOC area (the cyclonic circulation area where deep mixing and strong blooms occur seasonally). In the latter area, as known from literature, the bloom is subsequent to the early bloom initiation of the central and southern part of Western Mediterranean (Olita et al., 2011b). This was observed also in this case, despite the heat flux sign

inversion is contemporaneous for both the areas. So, heat fluxes, even if representing a good proxy for shutdown of the vertical turbulent convection (Bernardello et al., 2012) at interannual scales, do not seem a good indicator of the bloom onset at synoptic scales. Or, which is the same, they could work as indicator at all scales, but with different lags for different considered scales. It is probable that in the MEDOC area, as suggested by Chiswell (2011) for areas having a deep and well mixed upper layer, the assumption of an homogeneous distribution of phytoplankton would be effective and Sverdrup's CD hypothesis would be the best proxy for the bloom onset timing (instead of the CT hypothesis). Zeroing of heat fluxes in this case, even if diminishing the turbulent convection, did not imply a rapid re-stratification, nor the bloom initiation. The MEDOC area, even after the zeroing of heat fluxes, still shows the lower levels of Chl *a* over the whole basin because of its really deep ML, consequent to the sub-basin cyclonic circulation and to intense wind forcing often generating really deep ML and water cascades. On the contrary, the rapid re-stratification necessary for the early bloom initiation is possible, accordingly to Taylor and Ferrari (2011a), in presence of water masses of different densities close each other and dynamical features able to speed up such re-stratification process. Both the two conditions are present along the NBF, determinig the observed bloom initiation.

It is worth of notice that the southern winds event, that reached its maximum intensity on 4–5 March, was associated to the transport of desert dust from Saharian region into the western Mediterranean area. Aerosol Optical Thickness (AOT) L2 products from MODIS and correspondent quasi-true color images suggest the probable presence of dust in the atmosphere during the above mentioned period (not shown). The relation between atmospheric dust deposition (with its content in macro and micronutrients) and the blooming in Mediterranean was faced by several authors (Guerzoni et al., 1999, for a review). Authors pointed out that in NW Mediterranean the atmospheric nitrogen input could support up to $4\,C\,m^{-2}\,yr^{-1}$ while atmospheric phosphorus up to $1\,C\,m^{-2}\,yr^{-1}$. Despite this represents only 3–4 percent of total production in re-

spect to recent estimates (Olita et al., 2011b), it is suggested that episodic events could be triggered by such a deposition.

4 Summary and conclusions

Results show the triggering of phytoplankton bloom in correspondence of the shoaling of ML along the density front (North Balearic Front, NBF) between Balearic and Sardinia islands. Bloom initiation occurred because of the rapid re-stratification operated by the frontal instabilities after the shutdown of intense wind forcing and zeroing of heat fluxes (lowering of turbulent convection). A contribute in terms of increased input of nutrients during the pre-stratification period was also probable in virtue of large vertical velocities developing along fronts (Lévy et al., 2001; Lévy, 2008). Wind forcing, that was very intense during the 30–40 days of the glider cruise with many Mistral events, turned to be southward (warmer) in the last days of the cruise contributing to the inversion of the sign of heat fluxes (the sea started to warm) and the consequent lowering of turbulent convection. The after-storm re-stratification is found, as evidenced from glider data, to be faster just across the frontal area where lighter waters rapidly tend to overlay denser waters. The re-stratification is enhanced by the instabilities (meanders) of the front itself. This is not the case for areas far from the front. Another point of view of the observed phenomenon is that the breakthrough of the deep stratification in the frontal region, as shown in Fig. 3, could imply an enhanced supply of nutrient into the euphotic layers, considering that an intermediate barrier between sub-surface and deep layers was removed. This may play an additional role, in respect to the stratification of euphotic layers that is a necessary condition for the onset of the bloom, in promoting primary production.

Results of the present work suggest that such an early bloom of the southern area is actually due, as already hypothesized in the cited literature, to the mesoscale activity namely to the NBF and to the (margins of the) largest Anticyclonic Eddies.

We may also draw some general consideration about the onset of the bloom over the whole area. Satellite image for 9 March clearly shows the onset of the early bloom along the front, matched by the glider, and the extremely low concentration of Chl *a* in the MEDOC area: this is in agreement with previous findings (Olita et al., 2011a, b) showing a delay of about 1 month between early bloom in southern area and later and stronger bloom in the actual MEDOC area (north). This time-lag is compatible with the 3–4 weeks of bloom anticipation found by Mahadevan et al. (2012) in north Atlantic due to frontal processes. Considering the contemporaneous zeroing of heat fluxes throughout the basin and the asynchrony of the biological response of the different areas of the basin, it is clear that different processes trigger/enhance primary production for different scales/areas. In facts it seems that such a shutdown of turbulent convection would be effective only were the ML can shoal considerably by action of dynamical structures. In the deep ML area, where deep convection often occurs (Schroeder et al., 2008), there is not an immediate biological response to the zeroing of heat fluxes. We argue that in this area the classical CD hypothesis could be still a good approximation, in virtue of the deep mixing occurring in the area and of the supposedly homogeneous distribution of the phytoplankton throughout the ML (Chiswell, 2011). Heat fluxes zeroing is observed to precede by few days the bloom onset in the area where stratification is enhanced by frontal instabilities. Here the frontal-enhanced re-stratification mechanism described by Taylor and Ferrari (2011a) seems to be actual.

To verify some of the above speculations, the experimental approach could be implemented by operating a glider fleet in a wider area, even limited to a few hundred meters below the surface. Widening the observation will allow to clarify the mechanisms of blooms onset, which in turn will help to better understand phytoplankton dynamics acting at larger spatial and temporal scales over the whole Western Mediterranean sub-basin. Moreover, a combined modeling/observational study able to solve submesoscale would be needed to investigate the relative contribute of the enhanced biological pump and enhanced re-stratification to the onset of the early blooms in frontal areas.

The same experimental set-up, mainly based on high resolution quasi-synoptic sampling of the water column, could be applied to other Mediterranean regions, where existing fronts and associated submesoscale dynamics can play an important role in fertilizing the upper layer and triggering and sustaining observed seasonal blooms.

Acknowledgements. The research leading to results discussed in this paper has received funding by the European Union Seventh Framework Programme (FP7/2007-2013) under grant agreement no. 262584, JERICO. In particular, we especially thank the JERICO TNA program.

References

Behrenfeld, M. J.: Abandoning Sverdrup's Critical Depth Hypothesis on phytoplankton blooms, Ecology, 91, 977–989, 2010. 1560, 1561

Bernardello, R., Cardoso, J. G., Bahamon, N., Donis, D., Marinov, I., and Cruzado, A.: Factors controlling interannual variability of vertical organic matter export and phytoplankton bloom dynamics – a numerical case-study for the NW Mediterranean Sea, Biogeosciences, 9, 4233–4245, doi:10.5194/bg-9-4233-2012, 2012. 1561, 1569

Blumberg, A. and Mellor, G.: A description of a three-dimensional coastal ocean circulation model, in: Coastal Estuarine Science, edited by: Heaps, N. S., Am. Geophys. Union, Three-dimensional Coastal Ocean Models, 1–16, 1987. 1565

Castellari, S., Pinardi, N., and Leaman, K.: A model study of air-sea interaction in the Mediterranean Sea, J. Mar. Syst., 18, 89–114, 1998. 1565

Chiswell, S. M.: Annual cycles and spring blooms in phytoplankton: Don't abandon Sverdrup completely, Mar. Ecol.-Prog. Ser., 443, 39–50, 2011. 1561, 1569, 1571

Eriksen, C. C., Osse, T. J., Light, R. D., Wen, T., Lehman, T. W., Sabin, P. L., Ballard, J. W., and Chiodi, A. M.: Seaglider: A long-range autonomous underwater vehicle for oceanographic research, IEEE J. Ocean. Eng., 26, 424–436, 2001. 1563

Garau, B., Ruiz, S., Zhang, W. G., Pascual, A., Heslop, E., Kerfoot, J., and Tintoré.: Thermal lag correction on slocum CTD glider data, J. Atmos. Ocean. Technol., 28, 1065–1071, 2011. 1564

Guerzoni, S., Chester, R., Dulac, F., Herut, B., Loÿe-Pilot, M. D., Measures, C., Migon, C., Molinaroli, E., Moulin, C., Rossini, P., Saydam, C., Soudine, A., and Ziveri, P.: The role of

atmospheric deposition in the biogeochemistry of the Mediterranean Sea, Progr. Oceanogr., 44, 147–190, 1999. 1569

Huisman, J., van Oostveen, P., and Weissing, F.: Critical depth and critical turbulence: Two different mechanisms for the development of phytoplankton blooms, Limnol. Oceanogr., 44, 1781–1787, 1999. 1560, 1561

Kallos, G., Pytharoulis, I., and Katsafados, P.: Limited Area Weather Forecasting for the MF-STEP activities: Sensitivity and Performance Analysis, in: 4th EuroGOOS, Brest, France, 2005. 1565

Lévy, M.: The Modulation of Biological Production by Oceanic Mesoscale Turbulence, in: Transport and Mixing in Geophysical Flows, edited by: Weiss, J. and Provenzale, A., vol. 744 of Lecture Notes in Physics, 219–261, Springer Berlin/Heidelberg, 2008. 1562, 1570

Lévy, M., Klein, P., and Treguier, A.: Impact of sub-mesoscale physics on production and subduction of phytoplankton in an oligotrophic regime, J. Mar. Res., 59, 535–565, 2001. 1562, 1570

Lévy, M., Ferrari, R., Franks, P. J. S., Martin, A. P., and Riviere, P.: Bringing physics to life at the submesoscale, Geophys. Res. Lett., 39, L14602, doi:10.1029/2012GL052756, 2012. 1562

Mahadevan, A. and Tandon, A.: An analysis of mechanisms for submesoscale vertical motion at ocean fronts, Ocean Model., 14, 241–256, 2006. 1562

Mahadevan, A., D'Asaro, E., Lee, C., and Perry, M. J.: Eddy-driven stratification initiates North Atlantic spring phytoplankton blooms, Science, 336, 54–58, 2012. 1562, 1571

Martin, A.: The seasonal smorgasbord of the seas, Science, 336, 46–47, 2012. 1561

Millot, C. and Taupier-Letage, I.: Additional evidence of LIW entrainment across the Algerian subbasin by mesoscale eddies and not by a permanent westward flow, Progr. Oceanogr., 66, 231–250, doi:10.1016/j.pocean.2004.03.002, 2005. 1567

Olita, A., Ribotti, A., Sorgente, R., Fazioli, L., and Perilli, A.: SLA – chlorophyll-a variability and covariability in the Algero-Provençal Basin (1997–2007) through combined use of EOF and wavelet analysis of satellite data, Ocean Dynam., 61, 89–102, doi:10.1007/s10236-010-0344-9, 2011a. 1571

Olita, A., Sorgente, R., Ribotti, A., Fazioli, L., and Perilli, A.: Pelagic primary production in the Algero-Provençal Basin by means of multisensor satellite data: focus on interannual variability and its drivers, Ocean Dynam., 61, 1005–1016, doi:10.1007/s10236-011-0405-8, 2011b. 1568, 1570, 1571

Ribotti, A., Puillat, I., Sorgente, R., and Natale, S.: Mesoscale circulation in the surface layer off the southern and western Sardinia Island in 2000–2002, Chem. Ecol., 20, 345–363, 2004. 1566

Schroeder, K., Ribotti, A., Borghini, M., Sorgente, R., Perilli, A., and Gasparini, G. P.: An extensive western Mediterranean deep water renewal between 2004 and 2006, Geophys. Res. Lett., 35, L18605, doi:10.1029/2008GL035146, 2008. 1571

Sverdrup, H.: On conditions for the vernal blooming of phytoplankton, J. Cons. Int. Explor. Mer, 18, 287–295, 1953. 1561

Taylor, J. R. and Ferrari, R.: Ocean fronts trigger high latitude phytoplankton blooms, Geophys. Res. Lett., 38, L23601, doi:10.1029/2011GL049312, 2011a. 1560, 1562, 1568, 1569, 1571

Taylor, J. R. and Ferrari, R.: Shutdown of turbulent convection as a new criterion for the onset of spring phytoplankton blooms, Limnol. Oceanogr., 56, 2293–2307, doi:10.4319/lo.2011.56.6.2293, 2011b. 1560, 1561

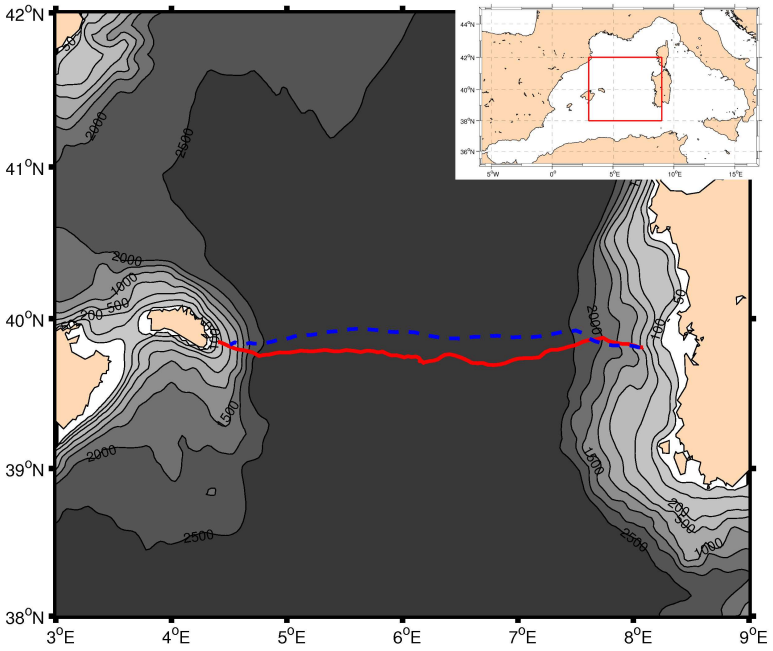

Fig. 1. Path of the glider overimpressed on the bathymetry of the Balearic Sea area. Outward (red) and return (blue) trips are represented.

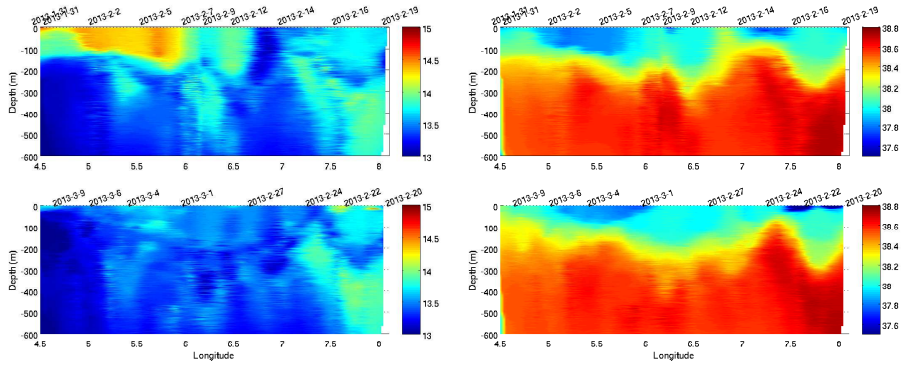

Fig. 2. Temperature (left) and salinity (right) zonal sections for outward (top panels) and return (bottom) glider trips. Dates are also indicated.

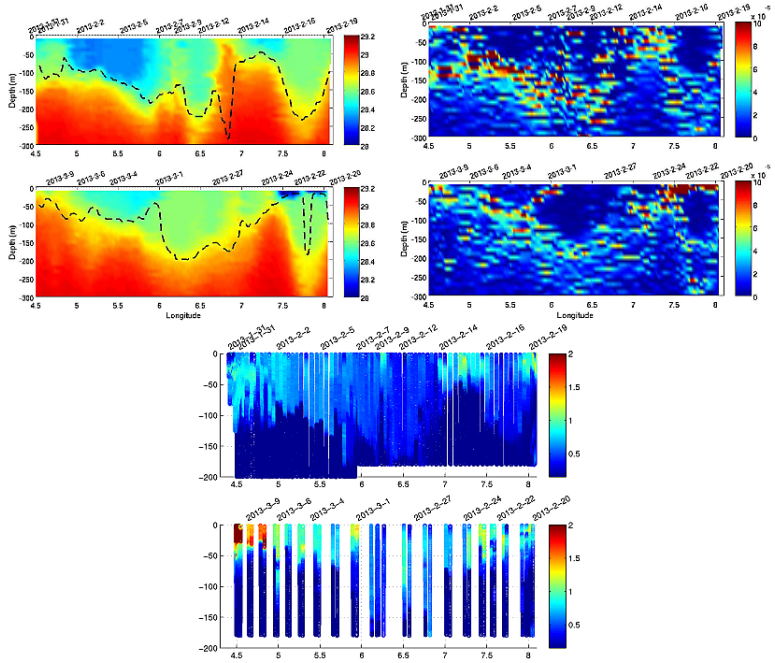

Fig. 3. Bottom: Chl *a* sections as observed from glider fluorimeter for outward (top) and return (bottom) trip. Top-left: MLD (density threshold criterion) as calculated from observed densities, overimposed on density section for outward and return trip. Top-right: Buoyancy (Brunt-Väisälä) frequency (s^{-2}).

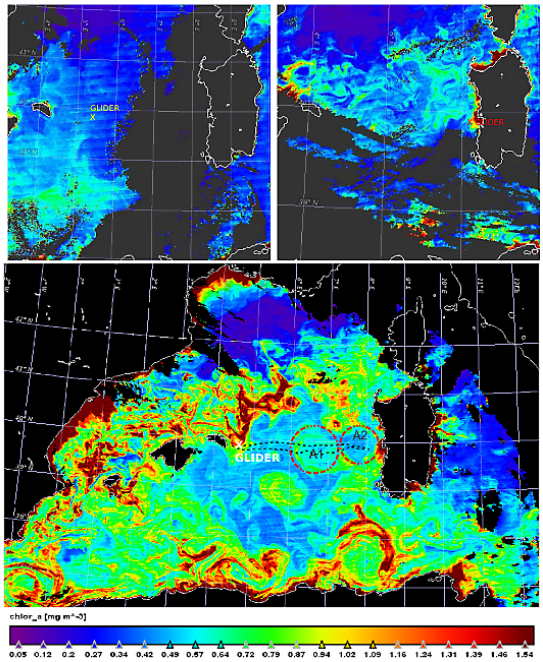

Fig. 4. Satellite AQUA MODIS Chl *a* concentration for: 4 February (top-left), 19 February (top-right) and 8 March (bottom), 2013. The occurrence of the bloom initiation along the whole front and along margins of the big Algerian Eddies is evident in the latter image. The position of the glider at the acquisition time is also superimposed on each image.

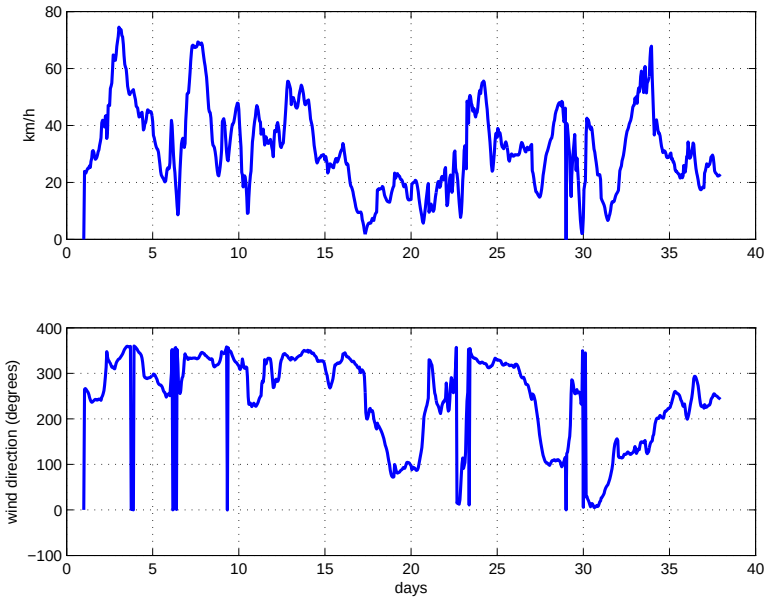

Fig. 5. Time series of the Skiron modeled hourly wind speed (top) and directions (bottom) for the period covered by the glider cruise. Direction values overpassing 300° correspond to mistral (NW) winds, while values ranging from 100 to 200° are southern winds.

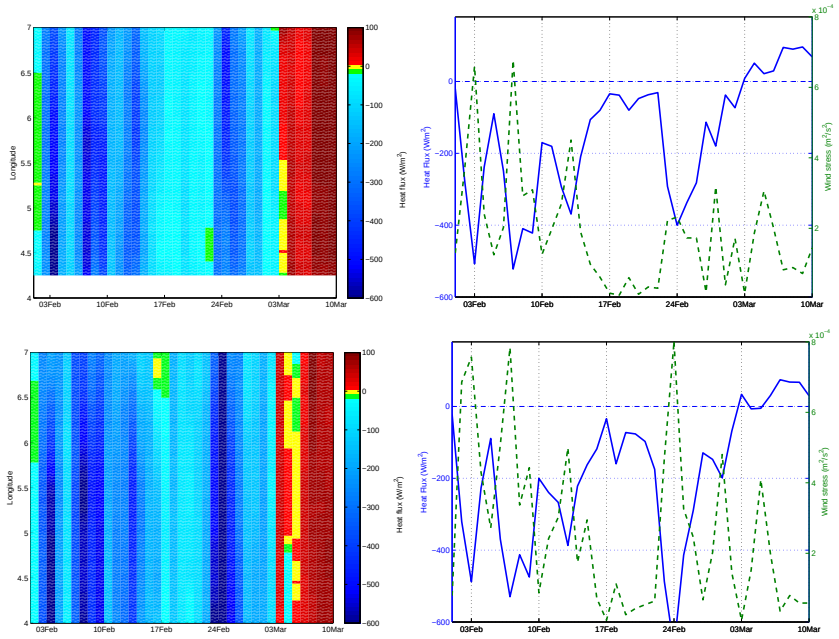

Fig. 6. Top panels: Hövmoller diagram (left panel) of heat fluxes along the glider path; wind stress and heat fluxes time series (right) averaged over the area covered by the glider path. Bottom: the same as top panels but at 42° N, thus north of the front and in the middle of the MEDOC area.